Highly siderophile element and ^{182}W evidence for a partial late veneer in the source of 3.8 Ga rocks from Isua, Greenland

Christopher W. Dale,[1*] Thomas S. Kruijer,[2] Kevin W. Burton[1]

[1] Department of Earth Sciences, Durham University, Durham, DH1 3LE, UK

[2] Institut für Planetologie, University of Münster, Wilhelm-Klemm-Str. 10, 48149 Münster, Germany

* Corresponding author: christopher.dale@durham.ac.uk

Abstract

The higher-than-expected concentrations of highly siderophile elements (HSE) in Earth's mantle most likely indicate that Earth received a small amount of late accreted mass after core formation had ceased, known as the 'late veneer'. Small ^{182}W excesses in the Moon and in some Archaean rocks – such as the source of 3.8 billion-year-old Isua magmatics – also appear consistent with the late veneer hypothesis, with a lower proportion received. However, ^{182}W anomalies can also relate to other processes, including early mantle differentiation. To better assess the origin of these W isotope anomalies – and specifically whether they relate to the late veneer – we have determined the HSE abundances and ^{182}W compositions of a suite of mafic to ultramafic rocks from Isua, from which we estimate HSE abundances in the source mantle and ultimately constrain the ^{182}W composition of the pre-late veneer mantle.

Our data suggest that the Isua source mantle had HSE abundances at around 50–65% of the present-day mantle, consistent with partial, but not complete, isolation from the late veneer. These data also indicate that at least part of the late veneer had been added and mixed into the mantle at the time the Isua source formed, prior to 3.8 Ga. For the same Isua samples we obtained a 13 ±4ppm ^{182}W excess, compared to the modern terrestrial mantle, in excellent agreement with previous data. Using combined ^{182}W and HSE data we show that the Moon, Isua, and the present-day bulk silicate Earth (BSE) produce a well-defined co-variation between ^{182}W composition and the mass fraction of late-accreted mass, as inferred from HSE abundances. This co-variation is consistent with the calculated effects of various late accretion compositions on the HSE and ^{182}W signatures of Earth's mantle. The empirical relationship, therefore, implies that the Moon, Isua source and BSE received increasing proportions of late-accreted mass, supporting the idea of disproportional late accretion to the Earth and Moon, and consistent with the interpretation that the lunar ^{182}W value of 27 ± 4 ppm represents the composition of Earth's mantle before the late veneer was added. In this case, the Isua source can represent ambient mantle after the giant moon-forming impact, into which only a part of Earth's full late veneer was mixed, rather than an isotopically distinct mantle domain produced by early differentiation, which would probably require survival through the giant Moon-forming impact.

1. Introduction

Late accretion is the period of material addition thought to follow the giant Moon-forming impact and the completion of core formation on Earth (e.g., Walker, 2009). The principal evidence for such late material addition comes from the concentrations of highly siderophile elements (HSE: e.g. Os, Pt, Re, Au) in Earth's mantle, which are higher than expected for metal-silicate equilibration during core formation (Brenan and McDonough, 2009; Mann et al., 2012). Moreover, the HSE in the mantle occur in broadly chondritic relative proportions, which is unexpected for metal-silicate partitioning (Meisel et al., 1996; Becker et al., 2006). These observations have led to the idea that the elevated HSE abundances in Earth's mantle reflect the late addition of broadly chondritic material (the 'late veneer') to the mantle after core formation was complete (e.g. Kimura et al., 1974).

Recently, the extinct ^{182}Hf-^{182}W decay system ($t_{1/2}$ = 8.9 Ma), which so far has mainly been used as a chronometer of core formation (Kleine et al., 2009), has emerged as a new tool with which to investigate late accretion (Willbold et al., 2011; Kruijer et al., 2015; Touboul et al., 2015; Willbold et al., 2015). During core formation, lithophile Hf separated from moderately siderophile W, causing Hf/W fractionation which, following decay of ^{182}Hf, led to distinct ^{182}W signatures in the mantle and core of planetary bodies. For instance, the present-day bulk silicate Earth (BSE) exhibits a higher ^{182}W/^{184}W by ~2 ε-unit (1ε = 0.01%) relative to chondrites, indicating that at least some part of Earth's core formed during the lifetime of ^{182}Hf (Kleine et al., 2002; Schoenberg et al., 2002; Yin et al., 2002; Kleine et al., 2004). The ^{182}W/^{184}W difference between Earth's mantle and chondrites not only provides constraints on the timing of core formation, but can also be used as a tracer of late-accreted material. This is because the addition of a late veneer with a composition and mass as inferred from HSE systematics lowered the ^{182}W/^{184}W of Earth's mantle by ~0.1 to ~0.4 ε-units (Willbold et al., 2011; Touboul et al., 2012; Kruijer et al., 2015; Touboul et al., 2015). Several recent studies have identified ^{182}W excesses of this magnitude in some Archaean samples and, in some cases, these signatures have been attributed to derivation of these samples from sources that lack some portion of the late veneer (Willbold et al., 2011; Willbold et al., 2015). However, the origin of these ^{182}W excesses is not fully understood and in other cases have been ascribed to very early differentiation events within Earth's mantle, rather than late accretion (Touboul et al., 2012; Touboul et al., 2014; Rizo et al., 2016).

One problem with the interpretation of the ^{182}W data is that until now no sample has been identified for which ^{182}W and HSE data provide consistent estimates for the amount of late-accreted material in the sample source. Elevated ε^{182}W of ~0.13 ($\varepsilon^{182}W = (^{182}W/^{184}W_{sample}/^{182}W/^{184}W_{terrestrial\ standard} - 1) \times 10^4$) in metabasalts and gneisses from the Isua supracrustal belt (ISB), Greenland, were attributed by Willbold et al. (2011) to an absence of late veneer, but HSE data, which would provide an

independent estimate, were not available. More recently, Rizo et al. (2016) used combined ^{182}W and HSE data for mafic and ultramafic rocks to argue that the ^{182}W enrichments in the Isua region were more likely produced by an early mantle differentiation event. Kostomuksha komatiites (Baltic Shield, Russia) have an $\varepsilon^{182}W$ excess of ~0.15, while Komati komatiites (Barberton greenstone belt, South Africa) have no resolvable excess, yet the HSE contents of these samples suggest that the fraction of late-accreted material in the Kostomuksha source is substantially higher than in the Komati source, inconsistent with a late accretion origin for the ^{182}W anomalies (Touboul et al., 2012). One possibility is that the HSE and ^{182}W systematics are decoupled, with W and HSE derived from different sources. For samples from the Nuvvuagittuq greenstone belt (Quebec, Canada), Touboul et al. (2014) argued for subduction-triggered addition of ^{182}W-enriched fluids to a mantle source containing the full complement of late-accreted material. The origin of the ^{182}W enrichment in these fluids remains unclear, however, and could be related to either a lower proportion of late veneer or early differentiation. In contrast, the constancy of ^{182}W excesses (~+0.15; Isua, Kostomuksha, Nuvvuagittuq and also Acasta), has been interpreted to reflect a global signature of a pre-late veneer mantle, enriched in HSE by giant impactor core material (Willbold et al., 2015). Recently, negative $\varepsilon^{182}W$ has been reported – the first such finding – in Schapenburg komatiites (Barberton greenstone belt) and this appears coupled with depletions in ^{142}Nd, suggesting a signature of early mantle differentiation (2016). Finally, elevated $\varepsilon^{182}W$ has been found for the first time in Phanerozoic samples (Rizo et al., 2016a), but the much larger magnitude of the anomaly (up to $\varepsilon^{182}W$ =+0.5 in Baffin Island picrites) is difficult to reconcile with any currently existing interpretations. Thus, overall, the origin of ^{182}W enrichments in terrestrial samples remains unclear and could either relate to late accretion, early differentiation, or both, or possibly even reflect heterogeneities produced during the main phase of accretion itself. Yet, while it is likely that at least some of the ^{182}W excesses observed for Archaean samples are due to late accretion, so far there is no single sample set for which this has been independently demonstrated.

Two recent studies have shown that the Moon exhibits an $\varepsilon^{182}W$ excess of ~0.22 to ~0.27 compared to the present-day BSE (Kruijer et al., 2015; Touboul et al., 2015). This excess is in good agreement with the ^{182}W difference expected for disproportional late accretion to the Earth and Moon and with the overall calculated effect of late accretion on the ^{182}W composition of Earth's mantle. These two studies, therefore, concluded that the ^{182}W composition of the Moon is indistinguishable from that of the pre-late veneer terrestrial mantle. This ^{182}W homogeneity is unexpected, however, given that the Moon is thought to consist of a mixture of impactor and proto-Earth material (e.g., Canup, 2004), both of which should be characterised by distinct ^{182}W compositions compared to the composition of Earth's mantle immediately after the giant impact (Kruijer et al., 2015). As such it is important to constrain the pre-late veneer ^{182}W composition of Earth's mantle without relying solely on the analyses of lunar samples. For example, if the lunar

^{182}W excess indeed represents the composition of the pre-late veneer BSE, then terrestrial samples with $\varepsilon^{182}W$ ~+0.15 should derive from mantle sources that contain about half of the late veneer.

Here we present combined HSE concentrations (Os, Ir, Ru, Pt, Pd, Re), ^{182}W and ^{187}Os data for 3.7-3.8 Ga samples from the Itsaq gneiss complex (south-west Greenland). The samples include pillow basalts and amphibolites from, respectively, the Isua supracrustal belt (ISB) and the adjacent orthogneiss terrain to the south (see Nutman and Friend, 2009) including several which have previously been identified as possessing ^{182}W excesses (Willbold et al., 2011). In addition, ^{182}W data and HSE concentrations are also presented for previously unstudied ultramafic rocks from the orthogneiss terrain, which arguably provide the most reliable estimate of mantle source HSE concentrations to date, as their major element composition and HSE proportions most closely approach those of the mantle itself. From these data we use the HSE concentrations to determine the proportion of late accretion received by the Isua mantle source, and combine this with W isotope data in order to place constraints on the formation of ^{182}W anomalies and the history of late accretion to Earth.

2. Samples and methods

2.1. Samples

Pillow basalts, amphibolites and ultramafic samples were collected from the early Archaean 3.7-3.8 Ga Itsaq gneiss complex, south-west Greenland, by Stephen Moorbath in 1998 and 2000. Pillow basalts were derived from the eastern arm of the Isua supracrustal belt (ISB) itself, while amphibolites and ultramafic rocks were sampled from numerous enclaves or pods in the adjacent ~3.8 Ga orthogneiss terrain to the south. Specifically, the ultramafic samples came from several enclaves just to the south of Lake 682 m (see Fig. 8 in Nutman and Friend, 2009), from the same region postulated to contain mantle dunites and harzburgites (Friend et al., 2002; Rollinson, 2007), although their exact origin remains unresolved. They are distinct from previously studied ultramafics in that they do not come from the ISB itself (cf. Szilas et al., 2015; Rizo et al., 2016), and they arguably provide the most robust mantle estimate due to their mantle-like HSE patterns. Three pillow basalts and one amphibolite have previously been analysed for ^{182}W, but not HSE (Willbold et al., 2011). In addition, data is also presented for two samples of younger 3.4 Ga Ameralik metadolerite dykes from within the Itsaq gneiss complex, collected by Robin Gill (localities RG24 and RG247). This provides a temporal constraint on the evolution of ^{182}W anomalies in this region.

Ultramafic rocks and amphibolites were taken from the low-strain areas of the orthogneiss terrain (Nutman and Friend, 2009), and although the amphibolites have experienced full recrystallisation

at amphibolite facies conditions, many samples, and the ultramafics in particular, display much less pervasive recrystallisation and, in particular, limited fluid flow and deformation. This has resulted in the preservation of pillow structures in the basalts and an almost complete absence of serpentinisation in the ultramafic samples (see supplementary petrographical material), reflected in low loss on ignition values of 0.8 to 2.2 wt. %. This, combined with mantle-like HSE patterns, is a key factor in interpreting the geochemical data presented here.

Some of the meta-pillow basalts and more pervasively deformed amphibolites have boninitic affinity, while most are tholeiitic as indicated by Al_2O_3/TiO_2 ratios of 15 or less (Szilas et al., 2015). In terms of HSE abundance patterns, as discussed further below, these show a notable similarity to some modern arc lavas, some of which also possess boninitic affinity. Ultramafic rocks from the ISB are typically thought to be cumulate rocks (Szilas et al., 2015). In particular, the combined MgO and NiO contents of olivines, and the Mg-poor, Cr-rich nature of their spinels, do not match the mantle range. However, unlike the ultramafic cumulates of the ISB (Szilas et al., 2015), the ultramafic lenses from the orthogneiss complex do not show any of the fractionation of HSE expected for cumulate rocks. Derivation by accumulation (e.g. from an HSE-poor melt) would almost certainly impart HSE fractionation (see figure 7 in Szilas et al., 2015 for Isua cumulate HSE patterns) due to the differing behaviour of Os, Ir and Ru over Pt and Pd during both the low degree of partial melting required to produce an HSE-poor melt, and during subsequent magmatic evolution and accumulation (e.g. Barnes et al., 1985). For instance, none of the cumulate samples from Isua (Szilas et al., 2015), and only one of 49 cumulates from Rum, Scotland (O'Driscoll et al., 2009) and Musk Ox, Canada (Day et al., 2008) has combined Pt/Os and Ir/(Pt+Pd) (Fig. S2) similar to the studied ultramafics, and that sample has strongly fractionated Os/Ir greater than 2.

A mantle origin is largely consistent with the typical mantle-like MgO (~35.5-38 wt.%; Table S1) and SiO_2 contents (44-46.5 wt.%), while the Al_2O_3 contents (3.9-5.5 wt.% for three of the four samples) are potentially slightly elevated due to secondary phlogopite and chlorite formation (e.g. Rollinson, 2007). Moreover, clear textural evidence for accumulation is lacking (see supplementary petrographical details). Only CaO contents diverge from a primitive mantle value (~ 3.5 wt. %) at 1-1.6 wt. %, reflecting the lack of clinopyroxene (Fig. S1). The major element compositions do, however, overlap with the ultramafic cumulates from the ISB (Szilas et al., 2015), making it difficult to rule out a cumulate origin. A further possibility is that rocks represent melt-reacted dunites, which can occasionally have low HSE abundances while maintaining relatively unfractionated HSE (e.g. Wang et al., 2013), but the rocks are too Al-rich, Mg-poor and have too much orthopyroxene to be dunites (Fig. S1). Meanwhile, a komatiitic origin is inconsistent with the low Ca contents (e.g. see Puchtel et al., 2007). Irrespective of their origin, the high Ni contents (Table S1), combined with the lack of HSE fractionation and MgO content, suggest minimal

fractionation, thus we believe these rocks provide the most robust opportunity to estimate the HSE concentrations of the Isua mantle source. .

2.2. Analytical methods

The analytical methods employed for HSE and Os isotope analysis follow closely those described in detail in Dale et al. (2012). Briefly, sample powders (~1.5 g) were digested and equilibrated with a mixed HSE spike using inverse aqua regia (16 mol l^{-1} HNO_3 and 12 mol l^{-1} HCl in 2:1 proportions) in quartz vessels heated in a high-pressure asher to 300°C for at least 17 hours. Osmium was extracted from the aqua regia using CCl_4 and then back extracted into 9 mol l^{-1} HBr (Cohen and Waters, 1996). This was then dried and microdistilled to further purify Os which was then loaded onto Pt filaments and analysed as OsO_3^- ions by thermal ionisation mass spectrometry on the secondary electron multiplier of a ThermoFinnigan Triton in negative mode, at Durham University. A DROsS standard solution (10-100 pg) gave the following mean value for the analytical periods of January-February 2012 and March 2013: $^{187}Os/^{188}Os$ = 0.16106 ± 0.00062 (n=16), in good agreement with a value of 0.160924 ± 4 on larger aliquots measured in Faraday cup mode (Luguet et al., 2008). The other HSE and Re were purified from the aqua regia solution using AGX1-8 anion exchange resin, and analysed on a ThermoFisher® Element 2 ICP-MS. Relevant standard solutions of HSE, Hf, Y, Zr, Mo and Cd were run at the start, during and end of the analytical session to correct for mass bias and isobaric interferences from oxide species (combined corrections <1% for Ir, Pt, Re and ~3% for Pd and Ru). The TDB-1 reference material gave the values in Table 1, in good agreement with those of a recent comprehensive analytical study (Ishikawa et al., 2014). Procedural blanks were typically insignificant (e.g. Os = 0.22 ± 0.17 pg; Pt = 4.1 ± 3.7 pg; Pd (the highest blank) = 30 ± 7.5 pg n=3, 2 s.d.) at <10% of all total measured elemental abundances, except for one low HSE sample (amphibolite SM/GR/00/26; up to 41% for Pd), and <1% for all ultramafic HSE analyses except Re (up to 5.5%).

The W isotope compositions were determined on powder aliquots (~0.5 g) of the same samples used for HSE analyses following the methods documented in Kruijer et al. (2015). In brief, after dissolution of the sample powders in HF–HNO_3, small (10%) solution aliquots were taken for determination of W concentrations by isotope dilution. Tungsten from the un-spiked samples was separated from the sample matrix using a two-stage anion exchange chromatography (Kruijer et al., 2015). Total procedural blanks were ~50-150 pg for the W isotope composition analyses, and insignificant given the amounts of W in the samples (W_{sample}/W_{blank} ≈ 400-7000). Tungsten isotope compositions were measured on a ThermoScientific® Neptune *Plus* MC-ICPMS at the University of Münster, following previously published protocols (Kruijer et al., 2015). All four major W isotopes (^{182}W, ^{183}W, ^{184}W, ^{186}W) were measured simultaneously in low-resolution mode using Jet sampler and X-skimmer cones. Total ion beams of ~2-3 $\times 10^{-10}$ A were obtained for ~30 ng/g W standard

solutions at an uptake rate of ~60 µl/min. A single W isotope measurement comprised a baseline followed by 200 cycles, each with a 4.2 s integration time. Small isobaric interferences from ^{184}Os and ^{186}Os on W isotope ratios were corrected by monitoring interference-free ^{188}Os, and were typically ~5-10 ppm on ε^{182}W, and always smaller than ~20 ppm. The ε^{182}W values reported have been corrected for instrumental mass bias by internal normalisation to ^{186}W/^{184}W = 0.92767 (denoted '6/4') using the exponential law (cf. Table S2 for correction using ^{186}W/^{183}W). The accuracy and reproducibility of the method were assessed through repeated analyses of terrestrial rock standards (BHVO-2, BCR-2, AGV-2) that were processed alongside the Isua samples. The W isotope analyses of samples were bracketed by measurements of terrestrial solution standards (Alfa Aesar) and results are reported as ε-unit (i.e., 0.01%) deviations from the mean values of the bracketing standards. The reported ε^{i}W in supplementary Table S1 represent the mean of pooled solution replicates (N = 4-10) together with the associated 95% confidence limits [i.e., according to (s.d. × $t_{95\%\ conf.,\ N-1}$)/√N]. This is justified given that the mean obtained for the terrestrial rock standards yields ε^{182}W (6/4) = 0.00±0.02 (95% conf., N = 37) (Kruijer et al., 2015), demonstrating that the W isotope measurements are accurate to a high level of precision.

3. Results

3.1. Highly siderophile elements

All samples display typical HSE patterns for their rock type (Fig. 1, Table 1), indicating that these elements, with the exception of Re, have not been significantly affected by low-temperature or metamorphic processes since emplacement. The basaltic samples have strongly fractionated HSE patterns, depleted in Os-Ir-Ru and slightly enriched in Pd and Pt with respect to primitive mantle (henceforth referred to as BSE), with high Pt/Ru ratios which bear resemblance to modern arc volcanics (Dale et al., 2012). The retention of very high Pt and Pd concentrations at relatively low MgO content (Fig. 2) is indicative of evolution of these melts under sulphur-undersaturated conditions as, otherwise, these elements would be strongly partitioned into precipitating sulphide ($D_{sul\text{-}sil\ liq}$ >100,000; Mungall and Brenan, 2014).

In contrast to the basaltic samples, ultramafic samples have broadly chondritic relative HSE abundances, with absolute concentrations that fall at the low end or below the range of modern-day peridotites, at 40 to 75% of the estimate for the BSE (Becker et al., 2006) (Figs. 1, 2 & 3). These ultramafics have Os concentrations (1.2 to 2.6 ng/g) comparable to a previous study of spinel peridotites south of Isua (Bennett et al., 2002). In detail, there is a similarity in HSE abundances and patterns with some of the oldest 3.4-3.5 Ga komatiite samples, from Barberton and Pilbara (Maier et al., 2009). The unfractionated HSE patterns of Isua ultramafics is a key feature when using these samples to estimate the HSE composition of the Isua mantle source.

The Isua ultramafic rocks studied also possess suprachondritic Ru/Ir and Pd/Ir ratios which are reminiscent of the estimated composition of BSE (Fig. 1) (Becker et al., 2006), and are higher than all known chondrite types. Given the debate on the interpretation and reliability of the BSE Ru/Ir and Pd/Ir fractionations (e.g. the role of metasomatism and residual platinum-group minerals; Lorand et al., 2010) we only speculatively note that this observed fractionation could relate either to the composition of late accreting material (Fischer-Gödde and Becker, 2012) or to a relict signature of partitioning between metallic/sulphide-rich core and silicate mantle (Laurenz et al., 2016). It might be expected that these scenarios would respectively result in less and more fractionated HSE patterns in a late veneer-poor Isua mantle. While the HSE fractionations in Isua ultramafics are possibly larger than BSE, any difference is not currently resolvable.

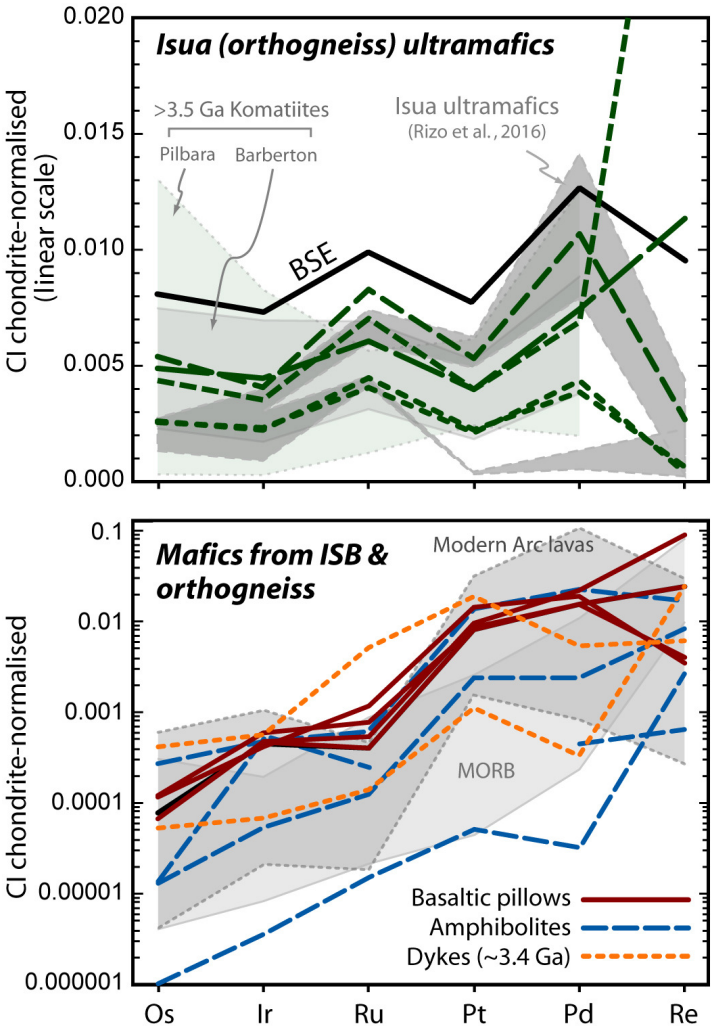

Fig. 1: Highly siderophile element concentrations in basaltic 'pillows' and ultramafic and amphibolite pods from the Isua supracrustal belt and adjacent orthogneiss terrain, normalised to CI chondrite. The basaltic and amphibolite samples bear a strong resemblance to some modern sulphide-undersaturated magmas, such as those from the Tonga arc. The ultramafics have broadly flat but slightly fractionated HSE patterns similar to 3.5 Ga Barberton komatiites and the PUM. PUM from Becker et al. (2006); komatiites: Maier et al.

(2009); Tonga arc lavas: Dale et al. (2012); MORB: Rehkämper et al. (1999); Bezos et al. (2005); Dale et al. (2008). CI values from Horan et al. (2003).

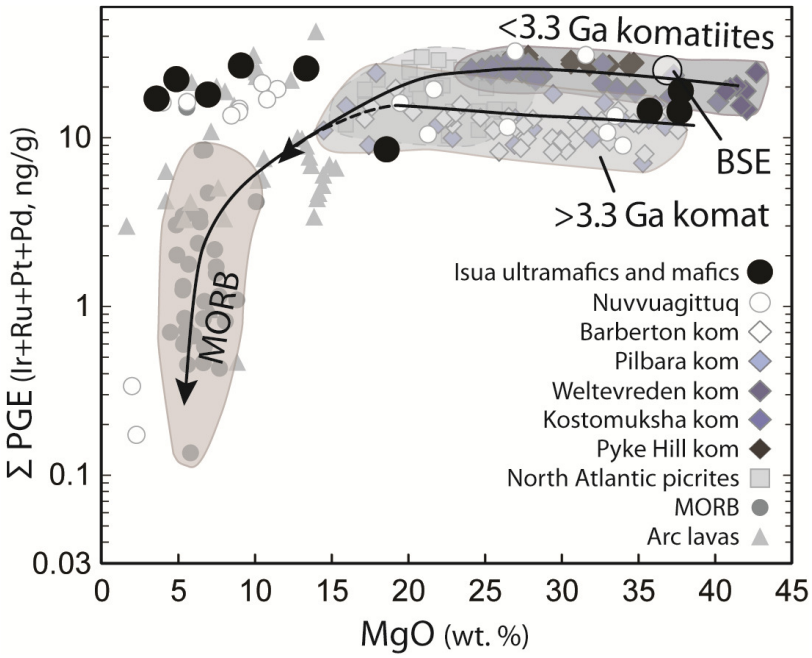

Fig. 2: Co-variation of MgO and HSE contents for compiled terrestrial mantle melts and Isua/Itsaq samples. Arrows denote approximate effect of sulphide-saturated magma differentiation from melts derived from post-3.3 Ga and pre- 3.3 Ga mantle sources. Note that on average post-3.3 Ga komatiites are distinctly more HSE-rich than those older than 3.3 Ga. High MgO ultramafic Isua samples plot between these two fields. Basaltic Isua samples have much higher HSE contents than MORB, but similar to modern-day arc samples, indicating sulphide undersaturated magma evolution (Dale et al., 2012). Such magma evolution makes it difficult to constrain the source HSE concentrations, but the data suggest a source which is approaching that of modern-day mantle and are consistent with the source defined by the ultramafics. Data sources: BSE – Becker et al. (2006); komatiites – Puchtel et al. (2004); Puchtel and Humayun (2005); Maier et al. (2009); Connolly et al. (2011); Nuvvuagittuq – Touboul et al. (2014); arc lavas – Woodland et al. (2002); Dale et al. (2012); MORB – Rehkämper et al. (1999); Bezos et al. (2005); Dale et al. (2008); Baffin and West Greenland plume-related picrites – Dale et al. (2009).

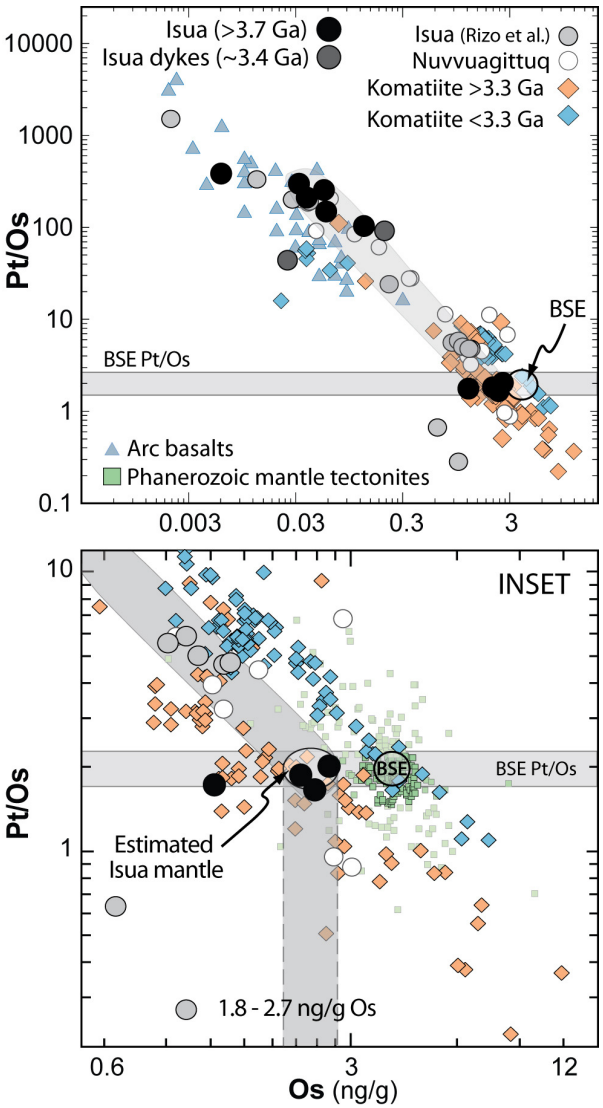

Fig. 3: Ratio of moderately compatible HSE (Pt) to highly compatible HSE (Os), plotted against the denominator. Data arrays for partial mantle melt suites approach the composition of the melt source at high degrees of partial melting. The Isua (orthogneiss-derived) ultramafic samples indicate a source with only 45-70% of the BSE Os content (defined by intersection of trend with Pt/Os range of BSE; lowest Os and MgO sample excluded). Recent data for ISB ultramafics (Rizo et al., 2016) are broadly consistent with this finding. As in figure 2, the HSE content of mafic samples is hard to interpret due to sulphide undersaturated evolution, but can be generated from such a source composition. For data sources see Fig. 2, additional data: mantle tectonites – references within Becker and Dale (2016); Volotsk and Schapenburg komatiites: Puchtel et al. (2007; 2009). Figure S3 shows the komatiite data by locality.

3.2. Tungsten isotopes

High-precision W isotope data for two mafic and three ultramafic samples from the Isua area are presented in Tables 1 and S2. The investigated samples include one pillow basalt for which there is previously published data, and one 3.4 Ga Ameralik dyke sample. All samples older than 3.7 Ga

have $\varepsilon^{182}W$ values that fall within uncertainty of each other, but are resolvably elevated compared to the modern mantle (Fig. 4). The average $\varepsilon^{182}W$ for the five >3.7 Ga samples is 0.13 ± 0.04 (95% conf.), identical to the mean from a previous study of mafic and felsic samples from Isua (Willbold et al., 2011). In addition, the data for sample SM/GR/98/26 is also in agreement with that of Willbold et al. (2011) (Fig. 4). The range of $\varepsilon^{182}W$ (~+0.05 to +0.20) found by Rizo et al. (2016), in different samples from the ISB itself, is also consistent with our data. In contrast, the younger dyke sample (3.4 Ga) does not have a resolvable ^{182}W excess, although the value also falls within uncertainty of most of the older samples. Conversely, Rizo et al. (2016) found 3.4 Ga samples to have indistinguishable $\varepsilon^{182}W$ from 3.7-3.8 Ga samples. There is no obvious analytical reason for this potential discrepancy, given our replicate data agree with those of Willbold et al. (2011), so we suggest this reflects the overall variability of each suite, as several 3.7-3.8 Ga samples from Rizo et al. (2016) also possess $\varepsilon^{182}W$ that is unresolvable from BSE.

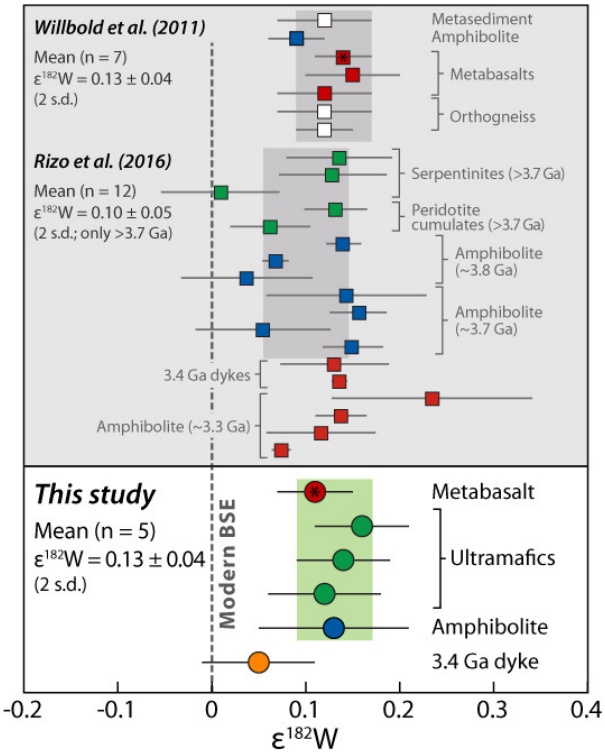

Fig. 4: The ^{182}W isotope composition of mafic and ultramafic rocks from the ISB and orthogneiss terrain, reported in parts per 10,000 deviation from a terrestrial standard. Our new data for > 3.7 Ga mafic and ultramafic samples are in excellent agreement with the data of Willbold et al. (2011), including one repeated sample, and those of Rizo et al. (2016). Most notably, the ultramafic samples which provide the most reliable estimates of mantle source HSE concentrations also possess indistinguishable positive $\varepsilon^{182}W$ anomalies. A younger 3.4 Ga Ameralik dyke sample has a $\varepsilon^{182}W$ composition which was not resolved from the modern mantle.

4. Discussion

4.1. A partial late veneer in the Isua source

Recent HSE-^{182}W data for the Isua region have been interpreted to reflect a near-complete late veneer component in the Isua mantle source (Rizo et al., 2016). Here we apply our new HSE data to this issue. The HSE data for our ultramafic lenses, and to some extent their major element contents, suggest that they might represent actual fragments of mantle, which would allow direct determination of mantle HSE concentrations (see Samples section and supplementary information for discussion). However, given that no current evidence is definitive, here we also consider that they could be primitive products of partial mantle melting. Thus, the HSE abundances in the Isua mantle source cannot be measured directly but must be derived from the concentrations measured in the igneous rocks. However, the low degree of fractionation of HSE in the ultramafic rocks, and their high MgO contents, results in the same mantle estimate whether or not a cumulate or direct mantle origin is assumed. Here we employ two methods to achieve a mantle source estimate (see also supplementary information): Firstly, HSE concentrations in igneous rocks co-vary with MgO content, thus enabling the concentration at typical mantle MgO to be determined and compared to other terrestrial mantle melts (Fig. 2). The second method uses ratios between two HSE of differing compatibility during mantle melting, plotted against the denominator, to define arrays for mantle melts which emanate from inter-element ratios and abundances that closely match those of the melt source (e.g. Figs. 3 and S3; in addition, the Ir/(Pt+Pd) ratio vs. Ir content is shown Fig. S2). For example, on a bulk scale, Pt is less compatible than Os during partial mantle melting, and so preferentially enters the melt. This gives high Pt/Os at low melt fractions but broadly chondritic Pt/Os and higher Os – approximating the mantle source – at very high melt fractions. Of the two methods, the ratio method should be more effective in taking into account differences in partitioning, source mineralogy and the crystallising assemblage, because such differences should result in variable gradients of the arrays rather than differences in apparent source composition. In comparison, MORB have massively different HSE contents to some arc lavas despite similar MgO, due to the effect of sulphide saturation in the former (Fig. 2). Both methods carry large uncertainties, particularly for low MgO, HSE-poor samples, but with the correct range of samples – particularly MgO-rich rocks approaching the composition of the mantle – constraints on mantle HSE content can still be obtained from either method. It should also be noted that using a number of different approaches, and assessing their consistency, is likely to produce the most robust estimates.

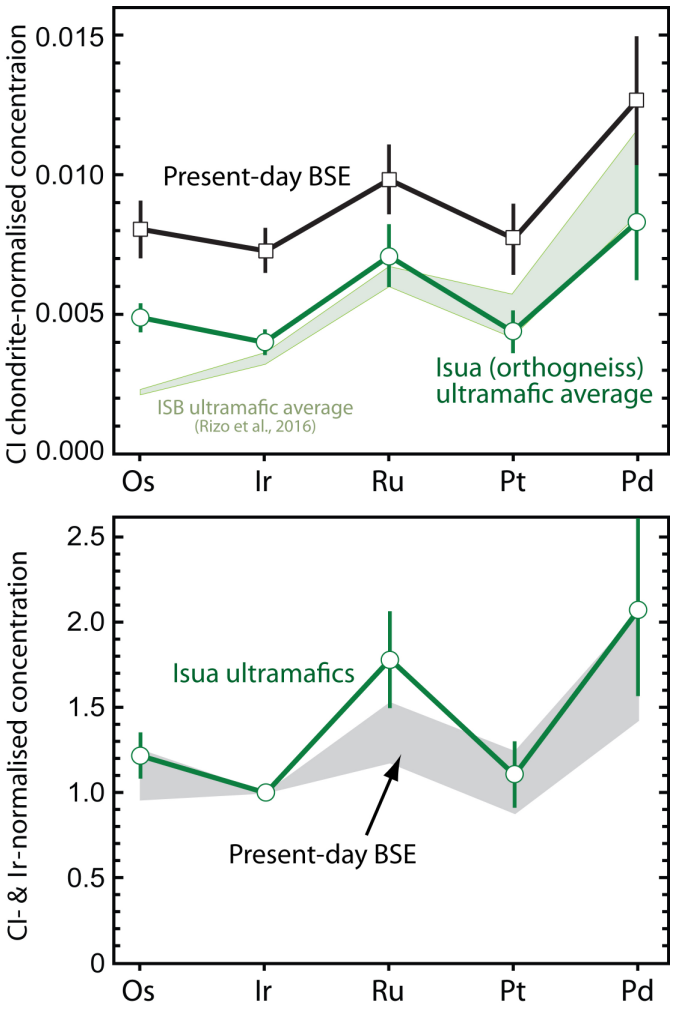

Fig. 5: HSE concentrations of Isua ultramafics (orthogneiss terrain) from this study compared with those estimated for the BSE. (a) CI chondrite-normalised HSE concentrations, and (b) CI-chondrite and Ir-normalised HSE concentrations. Also shown is the range of average HSE concentrations for ISB ultramafics from Rizo et al. (2016), where the upper values were calculated without the cumulate Pt- and Pd-depleted samples. HSE data for the BSE are from Becker et al. (2006). All uncertainties are at the 1σ, 68% confidence level. Two standard deviations produces a range of Os of 2.9 – 4.9 ng/g for BSE, and 1.95 – 2.8 ng/g for Isua ultramafics.

The ultramafic samples fall close to BSE in terms of MgO content and at or slightly below the BSE for Pt/Os ratio (and other HSE ratios). Thus, using the HSE ratio or the MgO method, it appears that their HSE contents are lower than expected for modern mantle-derived samples of the same MgO content or Pt/Os ratio; with a range of approximately 1.8 - 2.7 ng/g Os at the Pt/Os of BSE (Fig. 3). Due to the similarity of the ultramafic HSE ratios and the BSE (Fig. 5), the other HSE can be estimated to be present in the Isua source in similar proportions of the BSE value. Indeed, this allows estimation of the mantle value simply by the calculation of mean HSE concentrations in the ultramafic samples. The concentrations of Os, Ir, Ru, Pt and Pd are all between 49% and 65% of

the estimated BSE (Becker et al., 2006) with an average for all elements in the three most MgO-rich samples of 62±13% (2 s.d.). Due to the uncertainty behind the interpretation of the suprachondritic Ru/Ir and Pd/Ir ratios of Isua and BSE values, here we prefer to use only Os, Ir and Pt concentrations, which individually give ranges of 48-73% for Os, 42-68% for Ir and 37-77% for Pt (2 s.d.) compared to BSE, with averages of 60%, 55% and 57%, respectively. This gives an overall average for Os, Ir and Pt of 58% of BSE content, with an uncertainty on that average of ~6%. On this basis we conclude that the Isua source is deficient in HSE compared to the modern mantle and contains only ~52-64% of the full late veneer complement. These calculations inevitably produce specific figures, but it should be noted that the broader uncertainties (including the range of compositions found in the modern mantle) makes it difficult to categorically state the precise deficiency of HSE in the Isua mantle. Nonetheless, a comparison with mantle tectonites and high degree komatiitic melts (with equivalent Pt/Os) shows that only two out of 103 mantle samples, and no komatiites younger than 3.3 Ga, have Os concentrations as low as the Isua mantle range (Fig. 3 and Fig. S3). Only komatiites older than 3.3 Ga, for which an HSE-poor mantle source has been proposed (e.g. Maier et al., 2009; Puchtel et al., 2009; Connolly et al., 2011) fall within the Isua range for HSE ratios and concentrations. Thus, these data provide persuasive evidence that the Isua mantle source was significantly HSE-poor, probably between 50 and 65% of modern BSE.

This finding initially appears at odds with a recent conclusion of modern mantle-like HSE content in the Isua source, based on ultramafic rocks from the ISB itself (Rizo et al., 2016), rather than the orthogneiss terrain immediately to the south. While this cannot be entirely ruled out, a closer inspection reveals that the ultramafic samples in that study are broadly consistent with the HSE contents of the ultramafics presented here (Figs. 3, 4, 5). The reasons for the differing conclusions are two-fold. Firstly, and most notably, the ultramafic rocks in this study closely approach the mantle in HSE and major element composition, whereas those in Rizo et al. (2016) have somewhat fractionated HSE patterns, indicative of mantle melts, which require a greater degree of extrapolation to the mantle value. Secondly, the method of mantle HSE estimation differs, with Rizo et al. using a comparison of HSE patterns with modern samples and also Pt concentrations. The latter was based on the assumption that the concentration of Pt in the source is likely to be higher than the melt concentrations. Given that there are examples of mantle-derived rocks which have higher Pt concentrations than their assumed mantle sources (e.g. Rehkämper et al., 1999; Puchtel and Humayun, 2005; Dale et al., 2012), we believe this assumption is not supported (see supplementary information). If this requirement is not enforced then the average measured Pt concentration of the Rizo et al. samples is between 65 and 70% for both mafic and ultramafic samples – only ~10% higher than our estimate, despite their somewhat elevated Pt/Os ratios.

Furthermore, the data from Rizo et al. fall broadly within our Isua data array in Pt/Os vs. Os space (Fig. 3), consistent with a similar source HSE content.

Due to the difficulty in extrapolating from the less MgO-rich sulphide-undersaturated basaltic samples, we primarily base the HSE source estimate on the ultramafic samples. It should be noted, however, that the basaltic samples with high Pt and Pd concentrations can be produced from such a mantle source, as Pd and Pt behave incompatibly during sulphide-undersaturated fractional crystallisation and thus can be significantly enriched during magma evolution (e.g. Dale et al., 2012). Thus, our estimate for the late veneer fraction in the source of Isua ultramafics most likely applies to all >3.7 Ga Isua samples. As we will show below, this conclusion is consistent with the indistinguishable ^{182}W compositions of Isua mafic and ultramafic rocks.

4.2. Combined ^{182}W-HSE systematics – the effects of late accretion

Our HSE data suggest that the Isua source has not received the full complement of the late veneer, but that it is not completely devoid of late-accreted material. This raises the question of whether the observed HSE and ^{182}W constraints can both plausibly be accounted for by late accretion by providing mutually consistent estimates of the mass fraction of the late veneer present in the Isua source. To address this issue, we calculated the effect of late accretion on the ^{182}W composition of the BSE, to ultimately assess whether ~50-65% late veneer in the Isua source, as inferred from HSE systematics, is consistent with its ε^{182}W of ~0.13.

The effect of late accretion on the ^{182}W composition of Earth's mantle depends on the mass and composition of the late veneer. Although these can, in principle, be estimated using the absolute and relative abundances of HSE in Earth's mantle as well as its Se, Te and S systematics, no known composition easily accounts for all evidence presented. In particular, uncertainties regarding the interpretation of BSE estimates, the poorly known effects of core formation on ^{187}Os/^{188}Os and HSE ratios, and the realisation that we do not possess the full range of chondrite compositions present during late accretion, all currently preclude more definitive conclusions on the precise composition of the late veneer (Walker, 2009). Thus, here we investigate the effects on HSE and ^{182}W of a range of late veneer compositions including the major chondrite groups and also a minor fraction of differentiated, iron meteorite-like material (~20%).

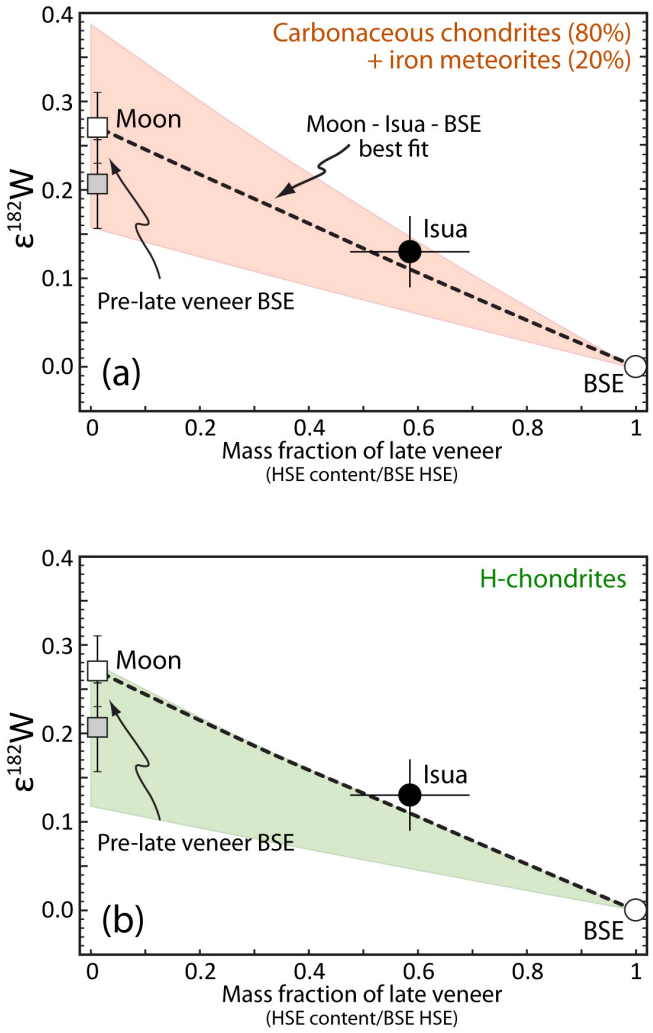

Fig. 6: ε^{182}W vs. mass fraction of late veneer. The data for the Moon, Isua and the present-day BSE exhibit a linear correlation (dashed lines; r^2=0.992). Also shown are mass balance calculations (shaded envelopes) for two late veneer compositions: (a) a mixture of carbonaceous chondrites (80%) and iron meteorites (20%), and (b) a purely H-chondrite-like late veneer. The uncertainty on the calculated pre-late veneer ^{182}W values mainly result from the uncertainty on the W concentration of the BSE (13±5 ng/g). Data for the Moon are from Kruijer et al. (2015) (*white square*) and Touboul et al. (2015) (*grey square*).

All chondrite groups and iron meteorites show deficits in ^{182}W relative to the BSE, so any late veneer would have added ^{182}W-depleted material to the BSE. Based on available W concentration and ^{182}W data (Yin et al., 2002; Kleine et al., 2004; Kleine et al., 2008; McCoy et al., 2011; Kruijer et al., 2014) and HSE data from the same samples (Table S3) (Horan et al., 2003; Fischer-Gödde et al., 2010), we calculate that subtracting an ordinary, enstatite or carbonaceous chondrite-like late veneer fraction *not* present in Isua's source (i.e., ~35-50%) from the present-day BSE composition would produce ε^{182}W excesses for Isua of $0.06^{+0.04}_{-0.02}$, slightly smaller than the observed

0.13 ± 0.04. However, Fig. 6 shows that Isua mantle, with a late veneer fraction of 0.50-0.65 and $\varepsilon^{182}W$ of 0.13 ± 0.04, plots well within the field calculated for the effect of a carbonaceous chondrite + iron meteorite late veneer on the ^{182}W composition of Earth's mantle, resulting in an $\varepsilon^{182}W$ of $0.09^{+0.06}_{-0.03}$. This is because the presence of iron meteorite material results in a higher W concentration (i.e., ~200 ng/g W) and larger ^{182}W-deficit (i.e., $\varepsilon^{182}W \approx -2.6$) than late veneer compositions exclusively composed of chondrites (~100-200 ng/g W; $\varepsilon^{182}W \approx -2$). Ordinary or enstatite chondrite material mixed with iron meteorites would also produce similar results. Of the pure chondrite compositions, without iron meteorite material, H-chondrites (metal-rich ordinary) have W and HSE systematics that most closely approach the late accretion effects of chondrite-iron mixtures (Fig. 6).

Thus, it is possible to reconcile the ^{182}W excess measured for Isua with its source containing a late veneer fraction of only ~50-65% as inferred from the HSE systematics of Isua ultramafic rocks. It should also be noted that the inclusion of iron meteorite material in this model is similar to the model of retention of some giant impactor core material in Earth's mantle, proposed by Willbold et al. (2015). That model also produces $\varepsilon^{182}W$ of ~0.13 at the HSE contents that we propose for the Isua mantle, if using an initial mantle value similar to that of the Moon (~0.25).

This is the first time that ^{182}W and HSE systematics for terrestrial samples provide mutually consistent estimates for the amount of late-accreted material in a mantle source. We note, however, that the modelled ^{182}W signature is strongly sensitive to the assumed W concentration of the present-day BSE, and this is reflected in the assigned uncertainty on the calculated ^{182}W value (shaded envelope in Fig. 6). Here we use a W concentration of 13±5 ppb for the BSE (2σ), which is based on its W/U ratio of 0.64±0.05 and assuming a U concentration for the BSE of 20±8 ppb (Arevalo and McDonough, 2008). An independent study using a range of ratios, including Ta/W, is also consistent with this estimate (12 ng/g W; König et al., 2011).

Although mixtures of chondritic (80%) and iron meteorite (20%) material produce the best matches to the Isua data, the calculated ^{182}W excesses produced by other late veneer compositions are well within uncertainty of both the measured ^{182}W signature of Isua and that calculated using mixed chondrite and iron meteorite compositions. This is because the assumed W concentration of the BSE exerts a strong control on the calculated effect of late accretion on $\varepsilon^{182}W$ and, moreover, the calculated late veneer percentage in BSE is somewhat coupled with the assumed late veneer composition. For example, a late veneer with relatively high HSE concentrations, high W concentration and low $\varepsilon^{182}W$ (e.g. H chondrite-like) would in principal have a larger effect on the ^{182}W signature of the BSE than a late veneer with lower HSE and W concentrations and higher $\varepsilon^{182}W$ (e.g. CI chondrite-like). Nevertheless, this effect is compensated by the higher late veneer fraction required in the BSE for CI compared to H chondrite veneers. Thus, changing the late

veneer composition does not lead to dramatically different calculated 'partial late veneer' ^{182}W compositions (Fig. 6).

4.3. Alternative mechanisms to account for ^{182}W-HSE systematics

Among the Archaean terranes so far investigated for high-precision W isotopes, the Isua source is unique in representing a mantle domain in which the coupled ^{182}W-HSE record set by partial late accretion appears to have been fully preserved. In contrast, the ^{182}W excesses observed for Kostomuksha komatiites (Touboul et al., 2012) and the Nuvvuagittuq greenstone belt (Touboul et al., 2014) are less easily attributed to a partial late veneer in their source, because their HSE contents suggest that their sources contained almost the entire complement of late veneer. Here we note, however, a similarity between Isua samples and some from Nuvvuagittuq in Figs. 2 & 3, perhaps suggesting that an HSE content notably lower than BSE is at least possible for the latter, but seems unlikely for Kostomuksha. Moreover, Schapenburg komatiites possess negative $\varepsilon^{182}W$ (Puchtel et al., 2016) and low HSE contents and is thus harder still to attribute to a partial veneer. It therefore seems likely that some of these ^{182}W excesses either do not reflect late accretion and are signatures of early differentiation of Earth's mantle or, alternatively, the W in these rocks derives from a different source than the HSE.

Decoupling of W and HSE could either be on the scale of a subduction flux, as proposed for Nuvvuagittuq (Touboul et al., 2014), or at a smaller scale whereby metamorphic fluids remobilised W. It should be noted that the consistent HSE patterns of the Isua samples (with the exception of Re) indicates that these elements have not been significantly mobilised since emplacement. Some Isua samples do, however, contain higher W concentrations than typically expected for their lithology (Table 1), which could be interpreted as subduction-related or post-magmatic enrichment of W, potentially imparting the ^{182}W enrichment (or reducing it). Nonetheless, all samples fall within the huge range of W concentrations of MORB and OIB (Figure S4) spanning two orders of magnitude to over 1 µg/g. While ultramafic samples might be expected to be lower in W than this range, the origin of variance in W concentration is not fully understood. Such variable concentrations and uncertainties regarding W behaviour during both igneous and fluid processes make firm conclusions regarding the W budget of Isua rocks problematic.

Many Isua samples have ratios of W/Th within the MORB/OIB and arc volcanics range (Fig. S5), while higher values could be interpreted as reflecting subduction-related addition of W. It should, however, be noted that Komati komatiites, for which a subduction origin has been excluded (Puchtel et al., 2014), have much higher W/Th. A partial melting or magmatic origin for elevated W/Th is not consistent with its negative co-variance with Th/Yb (Fig. S6a), given that the relative order of compatibility is W <Th << Yb (e.g. König et al., 2011); positive co-variance would be

predicted. A subduction-related origin might also be expected to show a positive covariation, due to the common enrichment of Th in arc lavas (Th flux may be dependent on the involvement of sediment, but W/U vs. U/Yb also shows the same relationship).

Despite differences in the precise behaviour of W and Ba during subduction, slab fluids tend to decrease the W/Ba ratio, while a slab melt flux leaves the ratio largely unchanged (König et al., 2011). Thus, if increasing W/Th reflects a slab-derived flux, then a negative co-variation, or a range of W/Th with little change in W/Ba would be predicted. In contrast, the Isua samples display a positive co-variation (Fig. S6b). Moreover, modern day arc volcanics do not show significantly higher W/Th than MORB and OIB (Fig. S4). It should be noted, however, that subduction-like systems in the Archaean probably possessed very different thermal regimes (e.g. Moyen and Martin, 2012) and thus modern constraints on elemental mobility in subduction zones may not be valid.

Recent work on Archaean rocks from Labrador, Canada, has found that in some cases the major phases do not account for the W content, which instead is distributed in phase boundary phases (Liu et al., 2016). This finding perhaps suggests that local remobilisation of W is the most likely explanation for elevated W/Th ratios in at least some samples. One alternative possibility is that the presence of elevated W/Th in Isua, Acasta, Komati and Nuvvuagittuq samples could reflect an inherent Archaean magmatic feature (Willbold et al., 2015), though no mechanism has yet been proposed.

In summary, the Isua W enrichments remain largely unexplained, but – notwithstanding significantly different mobility of W, Th and Ba under early Archaean conditions – large-scale subduction fluxing is not supported. It seems more likely that W enrichment is a local redistribution effect, but in this case the apparently systematic trace element behaviour (Fig. S6) seems somewhat surprising. Nonetheless, decoupling of W concentrations, and therefore potentially also ^{182}W, from the HSE cannot be ruled out. Yet, the widespread and constant ^{182}W signature in this region, suggests it relates to the whole terrane rather than having been sourced externally or from a particular rock type. It is also notable that samples which do not have higher-than-expected W contents (e.g. a mafic sample with 44 ng/g W), have ^{182}W enrichments identical to other samples which could arguably be enriched in W.

On balance, we conclude that without a fuller understanding of the behaviour of W in Archaean magmatic systems, subduction settings and metamorphic fluids, the mutually consistent estimates from ^{182}W and HSE for partial addition of the late veneer to the Isua source provides the simplest and most satisfactory explanation for the ^{182}W excess in Isua rocks relative to the modern mantle. Moreover, the widespread nature of the +0.13-0.15 $\varepsilon^{182}W$ anomaly (Isua, Kostomuksha, Nuvvuagittuq, Acasta and Labrador) is consistent with an ultimately late veneer origin for this

signature. In this case, the Isua mantle source represents ambient mantle, after the giant Moon-forming impact, into which a part of the late veneer was mixed. In comparison, a mantle differentiation origin (e.g. Touboul et al., 2012) requires an earlier process (pre-50 Ma; the effective lifespan of ^{182}Hf), which may predate the giant impact (>50 Ma; Halliday, 2008; Kruijer et al., 2015; Touboul et al., 2015). As it seems likely that at least some of the global ^{182}W anomalies reflect such early mantle differentiation (e.g. Touboul et al., 2012; Puchtel et al., 2016), one possibility is that the heterogeneous HSE-^{182}W data found in the komatiite record reflects an early, poorly-mixed lower mantle, while the Isua source represents the product of the giant-impact induced magma ocean. In this case, the preservation of ^{182}W anomalies generated by variable impactor compositions may also be a possible mechanism.

Nonetheless, in this scenario such lower mantle sources would have been preserved through large-scale impact melting of the silicate Earth (e.g. Canup, 2004; Cuk and Stewart, 2012) and, more importantly, their very small ^{182}W anomalies would have to be reconciled with the probability of a much larger change in ^{182}W as a result of a giant impact (most scenarios produce changes of >1 epsilon unit; Kleine et al., 2009).

4.4. Origin of the ^{182}W composition of the Moon

The coupled HSE-^{182}W evidence for a partial late veneer in the Isua source has important implications for understanding the ^{182}W composition of the Moon, and its consequences for constraining the late accretion history to the Earth and Moon. Two recent studies have shown that the Moon exhibits an ε^{182}W excess of 0.27±0.04 (Kruijer et al., 2015) or 0.21±0.05 (Touboul et al., 2015) over the present-day BSE. This ^{182}W excess is in good agreement with the predicted ε^{182}W change of $0.22^{+0.16}_{-0.07}$ resulting from the addition of a late veneer to Earth's mantle (calculated using the same late veneer mass and composition as used for Isua above). Based on this consistency both studies argued that the ^{182}W composition of the Moon reflects that of the pre-late veneer BSE. However, such ^{182}W homogeneity between BSE and Moon immediately following the giant impact is unexpected in current models of lunar origin (Kruijer et al., 2015). Moreover, processes other than late accretion may have been important in determining the ^{182}W composition of the Moon compared to that of Earth's mantle. For instance, the Moon may exhibit a small radiogenic ^{182}W excess relative to Earth's mantle, either inherited from the impactor or resulting from a higher Hf/W of the Moon compared to the BSE (Touboul et al., 2015). Moreover, as a result of early lunar differentiation, KREEP-rich rocks – on which the current estimate of the lunar ^{182}W composition is based – may be characterised by lower ε^{182}W compared to the bulk silicate Moon (Kleine et al., 2005). In light of these complexities it is crucial to independently constrain the ε^{182}W of the pre-late veneer BSE. The combined HSE-^{182}W data for Isua presented here provide such an opportunity.

A key observation from Fig. 6 is that the Moon, Isua and the present-day BSE define a single co-variation line, which is in very good agreement with the effects of late accretion on the ^{182}W composition of Earth's mantle as calculated using the late veneer compositions above. This empirical co-variation demonstrates that the ^{182}W differences observed between the Moon, Isua and the present-day BSE can all be attributed to variable portions of late-accreted material with mass fractions that are consistent with those inferred from HSE contents. The fact that the Moon, Isua and the present-day BSE plot close to one single correlation line leaves limited scope for an additional radiogenic ^{182}W signature in the Moon. As such, the Isua data presented here provide strong support for previous interpretations that the lunar $\varepsilon^{182}W$ reflects that of the pre-late veneer BSE (Kruijer et al., 2015; Touboul et al., 2015), which in turn provides supportive evidence for the interpretation that the HSE inventory of lunar rocks indicates an almost negligible amount of late-accreted mass added to the Moon (Day et al., 2007; Day and Walker, 2015). Collectively, these observations are best explained by disproportional late accretion to the Earth and Moon following the giant impact and the end of core formation on Earth (Day et al., 2007; Bottke et al., 2010; Day and Walker, 2015; Kruijer et al., 2015; Touboul et al., 2015).

5. Conclusions

Our results suggest that the Isua source mantle had HSE abundances at ~50-65% of the present-day mantle, consistent with partial isolation from the late veneer, but inconsistent with a complete absence of late accreted input (cf. Willbold et al., 2011). The combined HSE-W constraints for Isua, the Moon, and the present-day BSE reveal an empirical linear ^{182}W-HSE correlation that is consistent with mass balance calculations for the effect of late accretion on the W isotopic composition of Earth's mantle. Thus, these reservoirs probably received variable portions of late-accreted mass, supporting the idea of disproportional late accretion between the Earth and Moon. Together, this lends support to the interpretation that the 27±4 ppm ^{182}W excess of the Moon also represents the ^{182}W signature of Earth's earliest mantle, into which the late veneer was subsequently added. The Isua source, therefore, may represent ambient mantle postdating the giant impact that received only part of this late veneer, either because the remainder of the late veneer was added later or, perhaps more likely, not immediately thoroughly mixed into the whole of Earth's mantle.

Although the combined HSE-^{182}W data for Isua presented here demonstrate that partial late accretion leads to ^{182}W excesses, these data do not rule out a different origin for ^{182}W excesses observed in other terranes (e.g. Kostomuksha and Nuvvuagittuq; Touboul et al., 2012; 2014).

Acknowledgements

We are very grateful to Stephen Moorbath and Robin Gill for providing the samples used in this study. C.W.D. was supported by a Natural Environment Research Council Grant, NE/F005717/1 during part of this work. We thank Thorsten Kleine for considerable input which greatly improved an earlier version of this manuscript. We also thank Chris Ottley and Geoff Nowell for laboratory support in Durham. The detailed and thoughtful comments of three anonymous reviewers and Bernard Marty, the editor, have undoubtedly improved this manuscript substantially.

References

Arevalo, R., McDonough, W.F., 2008. Tungsten geochemistry and implications for understanding the Earth's interior. Earth and Planetary Science Letters 272, 656-665.

Barnes, S.-J., Naldrett, A.J., Gorton, M.P., 1985. The Origin of the Fractionation of Platinum-Group Elements in Terrestrial Magmas. Chemical Geology 53, 303-323.

Becker, H., Horan, M.F., Walker, R.J., Gao, S., Lorand, J.P., Rudnick, R.L., 2006. Highly siderophile element composition of the Earth's primitive upper mantle: Constraints from new data on peridotite massifs and xenoliths. Geochimica et Cosmochimica Acta 70, 4528-4550.

Becker, H., Dale, C.W., 2016. Re–Pt–Os Isotopic and Highly Siderophile Element Behavior in Oceanic and Continental Mantle Tectonites, in: Harvey, J., Day, J.M.D. (Eds.), Highly siderophile and strongly chalcophile elements in high temperature geochemistry and cosmochemistry. Mineralogical Society of America, Washington D.C., pp. 369-440.

Bennett, V.C., Nutman, A.P., Esat, T.M., 2002. Constraints on mantle evolution from Os-187/Os-188 isotopic compositions of Archean ultramafic rocks from southern West Greenland (3.8 Ga) and Western Australia (3.46 Ga). Geochimica et Cosmochimica Acta 66, 2615-2630.

Bezos, A., Lorand, J.P., Humler, E., Gros, M., 2005. Platinum-group element systematics in Mid-Oceanic Ridge basaltic glasses from the Pacific, Atlantic, and Indian Oceans. Geochimica et Cosmochimica Acta 69, 2613-2627.

Bottke, W.F., Walker, R.J., Day, J.M.D., Nesvorny, D., Elkins-Tanton, L., 2010. Stochastic Late Accretion to Earth, the Moon, and Mars. Science 330, 1527-1530.

Brenan, J.M., McDonough, W.F., 2009. Core formation and metal-silicate fractionation of osmium and iridium from gold. Nat. Geosci. 2, 798-801.

Canup, R.M., 2004. Dynamics of lunar formation. Annual Review of Astronomy and Astrophysics 42, 441-475.

Cohen, A.S., Waters, F.G., 1996. Separation of osmium from geological materials by solvent extraction for analysis by thermal ionisation mass spectrometry. Anal. Chim. Acta 332, 269-275.

Connolly, B.D., Puchtel, I.S., Walker, R.J., Arevalo, R., Piccoli, P.M., Byerly, G., Robin-Popieul, C., Arndt, N., 2011. Highly siderophile element systematics of the 3.3 Ga Weltevreden komatiites, South Africa: Implications for early Earth history. Earth and Planetary Science Letters 311, 253-263.

Cuk, M., Stewart, S.T., 2012. Making the Moon from a Fast-Spinning Earth: A Giant Impact Followed by Resonant Despinning. Science 338, 1047-1052.

Dale, C.W., Luguet, A., Macpherson, C.G., Pearson, D.G., Hickey-Vargas, R., 2008. Extreme platinum-group element fractionation and variable Os isotope compositions in Philippine Sea Plate basalts: Tracing mantle source heterogeneity. Chemical Geology 248, 213-238.

Dale, C.W., Pearson, D.G., Starkey, N.A., Stuart, F.M., Ellam, R.M., Larsen, L.M., Fitton, J.G., Macpherson, C.G., 2009. Osmium isotopes in Baffin Island and West Greenland picrites: Implications for the Os-187/Os-188 composition of the convecting mantle and the nature of high He-3/He-4 mantle. Earth and Planetary Science Letters 278, 267-277.

Dale, C.W., Macpherson, C.G., Pearson, D.G., Hammond, S.J., Arculus, R.J., 2012. Inter-element fractionation of highly siderophile elements in the Tonga Arc due to flux melting of a depleted source. Geochimica et Cosmochimica Acta 89, 202-225.

Day, J.M.D., Pearson, D.G., Taylor, L.A., 2007. Highly siderophile element constraints on accretion and differentiation of the Earth-Moon system. Science 315, 217-219.

Day, J.M.D., Pearson, D.G., Hulbert, L.J., 2008. Rhenium–osmium isotope and platinum-group element constraints on the origin and evolution of the 1· 27 Ga Muskox layered intrusion. Journal of Petrology 49, 1255-1295.

Day, J.M.D., Walker, R.J., 2015. Highly siderophile element depletion in the Moon. Earth and Planetary Science Letters 423, 114-124.

Fischer-Gödde, M., Becker, H., Wombacher, F., 2010. Rhodium, gold and other highly siderophile element abundances in chondritic meteorites. Geochimica et Cosmochimica Acta 74, 356-379.

Fischer-Gödde, M., Becker, H., 2012. Osmium isotope and highly siderophile element constraints on ages and nature of meteoritic components in ancient lunar impact rocks. Geochimica et Cosmochimica Acta 77, 135-156.

Friend, C., Bennett, V., Nutman, A., 2002. Abyssal peridotites> 3,800 Ma from southern West Greenland: field relationships, petrography, geochronology, whole-rock and mineral chemistry of dunite and harzburgite inclusions in the Itsaq Gneiss Complex. Contrib. Mineral. Petrol. 143, 71-92.

Halliday, A.N., 2008. A young Moon-forming giant impact at 70–110 million years accompanied by late-stage mixing, core formation and degassing of the Earth. Philosophical Transactions of the Royal Society of London A: Mathematical, Physical and Engineering Sciences 366, 4163-4181.

Horan, M.F., Walker, R.J., Morgan, J.W., Grossman, J.N., Rubin, A.E., 2003. Highly siderophile elements in chondrites. Chemical Geology 196, 5-20.

Ishikawa, A., Senda, R., Suzuki, K., Dale, C.W., Meisel, T., 2014. Re-evaluating digestion methods for highly siderophile element and ^{187}Os isotope analysis: evidence from geological reference materials. Chemical Geology 384, 27-46.

Kimura, K., Lewis, R.S., Anders, E., 1974. Distribution of gold and rhenium between nickel-iron and silicate melts - Implications for abundance of siderophile elements on Earth and Moon. Geochimica et Cosmochimica Acta 38, 683-701.

Kleine, T., Münker, C., Mezger, K., Palme, H., 2002. Rapid accretion and early core formation on asteroids and the terrestrial planets from Hf-W chronometry. Nature 418, 952-955.

Kleine, T., Mezger, K., Münker, C., Palme, H., Bischoff, A., 2004. ^{182}Hf-^{182}W isotope systematics of chondrites, eucrites, and Martian meteorites: Chronology of core formation and mantle differentiation in Vesta and Mars. Geochim. Cosmochim. Acta 68, 2935-2946.

Kleine, T., Palme, H., Mezger, K., Halliday, A.N., 2005. Hf-W chronometry of lunar metals and the age and early differentiation of the Moon. Science 310, 1671-1674.

Kleine, T., Touboul, M., Van Orman, J.A., Bourdon, B., Maden, C., Mezger, K., Halliday, A.N., 2008. Hf-W thermochronometry: Closure temperature and constraints on the accretion and cooling history of the H chondrite parent body. Earth and Planetary Science Letters 270, 106-118.

Kleine, T., Touboul, M., Bourdon, B., Nimmo, F., Mezger, K., Palme, H., Jacobsen, S.B., Yin, Q.Z., Halliday, A.N., 2009. Hf-W chronology of the accretion and early evolution of asteroids and terrestrial planets. Geochimica et Cosmochimica Acta 73, 5150-5188.

König, S., Münker, C., Hohl, S., Paulick, H., Barth, A.R., Lagos, M., Pfänder, J., Büchl, A., 2011. The Earth's tungsten budget during mantle melting and crust formation. Geochimica Et Cosmochimica Acta 75, 2119-2136.

Kruijer, T.S., Touboul, M., Fischer-Goedde, M., Bermingham, K.R., Walker, R.J., Kleine, T., 2014. Protracted core formation and rapid accretion of protoplanets. Science 344, 1150-1154.

Kruijer, T.S., Kleine, T., Fischer-Godde, M., Sprung, P., 2015. Lunar tungsten isotopic evidence for the late veneer. Nature 520, 534-537.

Laurenz, V., Rubie, D.C., Frost, D.J., Vogel, A.K., 2016. The importance of sulfur for the behavior of highly-siderophile elements during Earth's differentiation. Geochimica et Cosmochimica Acta 194, 123-138.

Liu, J., Touboul, M., Ishikawa, A., Walker, R.J., Pearson, D.G., 2016. Widespread tungsten isotope anomalies and W mobility in crustal and mantle rocks of the Eoarchean Saglek Block, northern Labrador, Canada: Implications for early Earth processes and W recycling. Earth and Planetary Science Letters 448, 13-23.

Lorand, J.P., Alard, O., Luguet, A., 2010. Platinum-group element micronuggets and refertilization process in Lherz orogenic peridotite (northeastern Pyrenees, France). Earth and Planetary Science Letters 289, 298-310.

Luguet, A., Nowell, G.M., Pearson, D.G., 2008. $^{184}Os/^{188}Os$ and $^{186}Os/^{188}Os$ measurements by Negative Thermal Ionisation Mass Spectrometry (N-TIMS): Effects of interfering element and mass fractionation corrections on data accuracy and precision. Chemical Geology 248, 342-362.

Maier, W.D., Barnes, S.J., Campbell, I.H., Fiorentini, M.L., Peltonen, P., Smithies, R.H., 2009. Progressive mixing of meteoritic veneer into the early Earth's deep mantle. Nature 460, 620-623.

Mann, U., Frost, D.J., Rubie, D.C., Becker, H., Audetat, A., 2012. Partitioning of Ru, Rh, Pd, Re, Ir and Pt between liquid metal and silicate at high pressures and high temperatures - Implications for the origin of highly siderophile element concentrations in the Earth's mantle. Geochimica et Cosmochimica Acta 84, 593-613.

McCoy, T.J., Walker, R.J., Goldstein, J.I., Yang, J., McDonough, W.F., Rumble, D., Chabot, N.L., Ash, R.D., Corrigan, C.M., Michael, J.R., Kotula, P.G., 2011. Group IVA irons: New constraints on the crystallization and cooling history of an asteroidal core with a complex history. Geochim. Cosmochim. Acta 75, 6821-6843.

Meisel, T., Walker, R.J., Morgan, J.W., 1996. The osmium isotopic composition of the Earth's primitive upper mantle. Nature 383, 517-520.

Moyen, J.-F., Martin, H., 2012. Forty years of TTG research. Lithos 148, 312-336.

Mungall, J.E., Brenan, J.M., 2014. Partitioning of platinum-group elements and Au between sulfide liquid and basalt and the origins of mantle-crust fractionation of the chalcophile elements. Geochimica et Cosmochimica Acta 125, 265–289.

Nutman, A.P., Friend, C.R.L., 2009. New 1:20,000 scale geological maps, synthesis and history of investigation of the Isua supracrustal belt and adjacent orthogneisses, southern West Greenland: A glimpse of Eoarchaean crust formation and orogeny. Precambrian Research 172, 189-211.

O'Driscoll, B., Day, J.M.D., Daly, J.S., Walker, R.J., McDonough, W.F., 2009. Rhenium-osmium isotopes and platinum-group elements in the Rum Layered Suite, Scotland: Implications for Cr-spinel seam formation and the composition of the Iceland mantle anomaly. Earth and Planetary Science Letters 286, 41-51.

Puchtel, I.S., Brandon, A.D., Humayun, M., 2004. Precise Pt-Re-Os isotope systematics of the mantle from 2.7-Ga komatiites. Earth and Planetary Science Letters 224, 157-174.

Puchtel, I.S., Humayun, M., 2005. Highly siderophile element geochemistry of Os-187-enriched 2.8 Ga Kostomuksha komatiites, Baltic shield. Geochimica et Cosmochimica Acta 69, 1607-1618.

Puchtel, I.S., Humayun, M., Walker, R.J., 2007. Os–Pb–Nd isotope and highly siderophile and lithophile trace element systematics of komatiitic rocks from the Volotsk suite, SE Baltic Shield. Precambrian Research 158, 119-137.

Puchtel, I.S., Walker, R.J., Anhaeusser, C.R., Gruau, G., 2009. Re-Os isotope systematics and HSE abundances of the 3.5 Ga Schapenburg komatiites, South Africa: Hydrous melting or prolonged survival of primordial heterogeneities in the mantle? Chemical Geology 262, 355-369.

Puchtel, I.S., Walker, R.J., Touboul, M., Nisbet, E.G., Byerly, G.R., 2014. Insights into early Earth from the Pt–Re–Os isotope and highly siderophile element abundance systematics of Barberton komatiites. Geochimica et Cosmochimica Acta 125, 394-413.

Puchtel, I.S., Blichert‐Toft, J., Touboul, M., Horan, M.F., Walker, R.J., 2016. The coupled 182W‐142Nd record of early terrestrial mantle differentiation. Geochemistry, Geophysics, Geosystems.

Rehkämper, M., Halliday, A.N., Fitton, J.G., Lee, D.C., Wieneke, M., Arndt, N.T., 1999. Ir, Ru, Pt, and Pd in basalts and komatiites: New constraints for the geochemical behavior of the platinum-group elements in the mantle. Geochimica et Cosmochimica Acta 63, 3915-3934.

Rizo, H., Walker, R.J., Carlson, R.W., Touboul, M., Horan, M.F., Puchtel, I.S., Boyet, M., Rosing, M.T., 2016. Early Earth Differentiation Investigated Through ^{142}Nd, ^{182}W, and Highly Siderophile Element Abundances in Samples From Isua, Greenland. Geochimica et Cosmochimica Acta 175, 319-336.

Rollinson, H., 2007. Recognising early Archaean mantle: a reappraisal. Contrib. Mineral. Petrol. 154, 241-252.

Schoenberg, R., Kamber, B.S., Collerson, K.D., Eugster, O., 2002. New W-isotope evidence for rapid terrestrial accretion and very early core formation. Geochimica et Cosmochimica Acta 66, 3151-3160.

Szilas, K., Kelemen, P.B., Rosing, M.T., 2015. The petrogenesis of ultramafic rocks in the > 3.7 Ga Isua supracrustal belt, southern West Greenland: Geochemical evidence for two distinct magmatic cumulate trends. Gondwana Research 28, 565-580.

Touboul, M., Puchtel, I.S., Walker, R.J., 2012. W-182 Evidence for Long-Term Preservation of Early Mantle Differentiation Products. Science 335, 1065-1069.

Touboul, M., Liu, J.G., O'Neil, J., Puchtel, I.S., Walker, R.J., 2014. New insights into the Hadean mantle revealed by W-182 and highly siderophile element abundances of supracrustal rocks from the Nuvvuagittuq Greenstone Belt, Quebec, Canada. Chemical Geology 383, 63-75.

Touboul, M., Puchtel, I.S., Walker, R.J., 2015. Tungsten isotopic evidence for disproportional late accretion to the Earth and Moon. Nature 520, 530-533.

Walker, R.J., 2009. Highly siderophile elements in the Earth, Moon and Mars: Update and implications for planetary accretion and differentiation. Chemie Der Erde-Geochemistry 69, 101-125.

Wang, Z.C., Becker, H., Gawronski, T., 2013. Partial re-equilibration of highly siderophile elements and the chalcogens in the mantle: A case study on the Baldissero and Balmuccia peridotite massifs (Ivrea Zone, Italian Alps). Geochimica Et Cosmochimica Acta 108, 21-44.

Willbold, M., Elliott, T., Moorbath, S., 2011. The tungsten isotopic composition of the Earth's mantle before the terminal bombardment. Nature 477, 195-191.

Willbold, M., Mojzsis, S.J., Chen, H.W., Elliott, T., 2015. Tungsten isotope composition of the Acasta Gneiss Complex. Earth and Planetary Science Letters 419, 168-177.

Woodland, S.J., Pearson, D.G., Thirlwall, M.F., 2002. A platinum group element and Re-Os isotope investigation of siderophile element recycling in subduction zones: Comparison of Grenada, Lesser Antilles arc, and the Izu-Bonin arc. Journal of Petrology 43, 171-198.

Yin, Q.Z., Jacobsen, S.B., Yamashita, K., Blichert-Toft, J., Telouk, P., Albarede, F., 2002. A short timescale for terrestrial planet formation from Hf-W chronometry of meteorites. Nature 418, 949-952.

Table 1. HSE concentrations and Os isotopes in ultramafic, mafic (pillow basalt) and amphibolitic samples from the Isua supracrustal belt and adjacent orthogneiss complex, Southwest Greenland.

	Sample mass	MgO	$\varepsilon^{182}W$	2 s.e.	W	Os^{α}	Os	Ir	Ru	Pt	Pd	Re	$^{187}Os/^{188}Os$		$^{187}Re/$	$\gamma Os^{\#}$
		wt.%			ng/g	ng/g	ng/g	ng/g	ng/g	ng/g	ng/g	ng/g			^{188}Os	(3.8 Ga)
Ultramafics (3.7-3.8 Ga)																
SMGR/00/12	1.507	18.58	0.16	**0.10**	129	1.245	**1.245**	1.05	3.16	2.18	2.14	0.022	0.11014	(12)	0.086	3.8
rpt	1.501	-				1.224	**1.224**	1.11	2.86	2.04	2.42	0.013	0.10899	(20)	0.049	5.0
SMGR/00/24	1.502	37.25	0.16	**0.07**	286	2.607	**2.607**	1.94	5.88	5.23	5.97	0.097	0.11878	(12)	0.178	6.4
SMGR/00/27	1.509	35.72	0.12	**0.07**	318	2.363	**2.376**	2.13	4.29	3.91	4.15	0.413	0.16999	(06)	0.841	14.2
SMGR/00/29	1.504	37.66	-	-	325	2.102	**2.170**	1.68	4.99	3.93	3.83	1.29	0.37064	(14)	2.96	76.2
Pillow basalts (3.7-3.8 Ga)																
SMGR/98/21	1.520	13.33	*0.12*	*0.05*	44	0.057	**0.064**	0.200	-	14.14	10.59	0.127	1.1609	(15)	10.79	352.7
SMGR/98/23	1.471	6.92	*0.15*	*0.05*	167	0.059	**0.066**	0.284	0.549	8.55	8.65	0.147	1.0367	(5)	12.07	146.3
SMGR/98/26	1.506	3.58	0.11	**0.03**	213	0.038	**0.079**	0.213	0.285	8.01	8.61	0.883	8.359	(2)	111.88	939.9
			0.14	*0.03*												
SMGR/98/35	1.505	4.85	-	-	521	0.033	**0.149**	0.228	0.379	9.43	12.28	3.26	28.71	(9)	500.48	-4066
Amphibolites (3.7-3.8 Ga)																
SMGR/00/17	1.502	9.07	0.14	**0.10**	326	0.133	**0.154**	0.228	0.438	13.60	12.59	0.611	1.3676	(11)	22.14	-178.7
SMGR/00/22	1.504	7.29	*0.09*	*0.03*	189	0.007	**0.008**	0.254	0.178	-	0.250	0.024	1.5597	(13)	16.12	402.5
rpt	1.503	-	-	-		0.006	**0.011**	0.026	0.089	2.37	1.34	0.305	6.102	(5)	232.01	-9097
SMGR/00/26	1.504	-	-	-	455	0.001	**0.004**	0.002	0.011	0.05	0.018	0.094	62.69	(8)	988.91	-2026
Ameralik dykes (~3.4 Ga)																
242631	1.041	-	-	-	154	0.204	**0.211**	0.272	3.64	18.77	2.99	0.223	0.3977	(3)	0.0534	5.27
242774	1.504	-	0.05	**0.06**	148	0.026	**0.054**	0.033	0.100	1.11	0.185	0.892	8.566	(8)	-2.416	168.0
Reference materials [γ]																
TDB-1	1.01	-					**0.104**	0.059	0.188	4.63	24.7	-	0.9688	(3)		
TDB-1	1.00	-					**0.120**	0.063	0.195	4.92	22.5	-	0.9359	(9)		
TDB-1	1.01	-					**0.117**	0.067	0.206	4.89	24.5	-	0.9076	(3)		
TDB-1	1.00	-					-	0.061	0.251	5.82	21.9	0.98	-		-	
TDB-1	1.00	-					**0.094**	0.056	0.258	4.43	21.5	1.00	1.0531	(3)	57.8	
TDB-1	1.00	-					**0.103**	0.059	0.296	4.65	22.4	1.07	0.9733	(4)	55.2	
TDB-1	1.00	-					**0.100**	0.050	0.221	3.86	18.9	1.00	1.0633	(2)	53.9	

NOTES:
$^{182}W/^{184}W$ compositions are given as $\varepsilon^{182}W$: ε is the deviation from the present-day silicate Earth, in parts per 10,000 [$\varepsilon^{182}W = ((^{182}W/^{184}W_{sample})/(^{182}W/^{184}W_{present\ mantle})-1)*10000$]. $\varepsilon^{182}W$ values in grey italics from Willbold et al. (2011). $^{\alpha}$ – Common Os, after subtraction of radiogenic ^{187}Os, based on the calculated initial Os isotope composition at 3.8 Ga (the age of igneous crystallisation). * - Initial $^{187}Os/^{188}Os$ corrected for ingrowth of ^{187}Os. $^{\gamma}$ Ref. material data from 3 year period, encompassing analytical period (see also Ishikawa et al., 2014).